Chapter 8

The Planetary Boundary Layer

The *planetary boundary layer* is that portion of the atmosphere in which the flow field is strongly influenced directly by interaction with Earth's surface. Ultimately this interaction depends on molecular viscosity. It is, however, only within a few millimeters of the surface, where vertical shears are very intense, that molecular diffusion is comparable to other terms in the momentum equation. Outside this *viscous sublayer* molecular diffusion is not important in the boundary layer equations for the mean wind, although it is still important for small-scale turbulent eddies. However, viscosity still has an important indirect role; it causes the velocity to vanish at the surface. As a consequence of this *no-slip boundary condition,* even a fairly weak wind will cause a large-velocity shear near the surface, which continually leads to the development of turbulent eddies.

These turbulent motions have spatial and temporal variations at scales much smaller than those resolved by the meteorological observing network. Such shear-induced eddies, together with convective eddies caused by surface heating, are very effective in transferring momentum to the surface and transferring heat (latent and sensible) away from the surface at rates many orders of magnitude faster than can be done by molecular processes. The depth of the planetary boundary layer produced by this turbulent transport may range from as little as 30 m in conditions of large static stability to more than 3 km in highly convective conditions. For average midlatitude conditions the planetary boundary layer extends through the lowest kilometer of the atmosphere and thus contains about 10% of the mass of the atmosphere. Given the modest vertical displacement of air parcels, we apply the Boussinesq approximation of Section 2.8 in subsequent analysis.

The dynamical structure of the flow in the planetary boundary layer is not produced directly by viscosity. Rather, it is largely determined by the fact that the atmospheric flow is turbulent. In the *free atmosphere* (i.e., the region above the planetary boundary layer), this turbulence can be ignored in an approximate treatment of synoptic-scale motions, except perhaps in the vicinity of jet

An Introduction to Dynamic Meteorology. DOI: 10.1016/B978-0-12-384866-6.00008-8

streams, fronts, and convective clouds. However, in the boundary layer the dynamical equations of the previous chapters must be modified to properly represent the effects of turbulence.

8.1 ATMOSPHERIC TURBULENCE

Turbulent flow contains irregular quasi-random motions spanning a continuous spectrum of spatial and temporal scales. Such eddies cause nearby air parcels to drift apart and thus mix properties such as momentum and potential temperature across the boundary layer. Unlike the large-scale rotational flows discussed in earlier chapters, which have depth scales that are small compared to their horizontal scales, the turbulent eddies of concern in the planetary boundary layer tend to have similar scales in the horizontal and vertical. The maximum eddy length scale is thus limited by the boundary layer depth to be about 10^3 m. The minimum length scale (10^{-3} m) is that of the smallest eddies that can exist in the presence of diffusion by molecular friction.

Even when observations are taken with very short temporal and spatial separations, a turbulent flow will always have scales that are unresolvable because they have frequencies greater than the observation frequency and spatial scales smaller than the scale of separation of the observations. Outside the boundary layer, in the free atmosphere, the problem of unresolved scales of motion is usually not a serious one for the diagnosis or forecasting of synoptic- and larger-scale circulations (although it is crucial for the mesoscale circulations discussed in Chapter 9). The eddies that contain the bulk of the energy in the free atmosphere are resolved by the synoptic network. However, in the boundary layer, unresolved turbulent eddies are of critical importance. Through their transport of heat and moisture away from the surface, they maintain the surface energy balance, and through their transport of momentum to the surface, they maintain the momentum balance. The latter process dramatically alters the momentum balance of the large-scale flow in the boundary layer so that geostrophic balance is no longer an adequate approximation to the large-scale wind field. It is this aspect of boundary layer dynamics that is of primary importance for dynamical meteorology.

8.1.1 Reynolds Averaging

In a turbulent fluid, a field variable such as velocity measured at a point generally fluctuates rapidly in time as eddies of various scales pass the point. In order that measurements be truly representative of the large-scale flow, it is necessary to average the flow over an interval of time long enough to average out small-scale eddy fluctuations, but still short enough to preserve the trends in the large-scale flow field. To do this we assume that the field variables can be separated into slowly varying mean fields and rapidly varying turbulent components. Following the scheme introduced by Reynolds, we then assume that for

any field variables, w and θ, for example, the corresponding means are indicated by overbars and the fluctuating components by primes. Thus, $w = \overline{w} + w'$ and $\theta = \overline{\theta} + \theta'$.

By definition, the means of the fluctuating components vanish; the product of a deviation with a mean also vanishes when the time average is applied. Thus,

$$\overline{w'\overline{\theta}} = \overline{w'}\,\overline{\theta} = 0$$

where we have used the fact that a mean variable is constant over the period of averaging. The average of the product of deviation components (called the *covariance*) does not generally vanish. Thus, for example, if on average the turbulent vertical velocity is upward where the potential temperature deviation is positive, and downward where it is negative, the product $\overline{w'\theta'}$ is positive and the variables are said to be correlated positively.

These averaging rules imply that the average of the product of two variables will be the product of the average of the means plus the product of the average of the deviations:

$$\overline{w\theta} = \overline{(\overline{w} + w')(\overline{\theta} + \theta')} = \overline{w}\overline{\theta} + \overline{w'\theta'}$$

Before applying the Reynolds decomposition to the Boussinesq equations (2.56) through (2.59), it is convenient to rewrite the total derivatives in each equation in flux form. For example, the term on the left in (2.56) may be manipulated with the aid of the continuity equation (2.60) and the chain rule of differentiation to yield

$$\begin{aligned}\frac{Du}{Dt} &= \frac{\partial u}{\partial t} + u\frac{\partial u}{\partial x} + v\frac{\partial u}{\partial y} + w\frac{\partial u}{\partial z} + u\left(\frac{\partial u}{\partial x} + \frac{\partial v}{\partial y} + \frac{\partial w}{\partial z}\right)\\ &= \frac{\partial u}{\partial t} + \frac{\partial u^2}{\partial x} + \frac{\partial uv}{\partial y} + \frac{\partial uw}{\partial z}\end{aligned} \tag{8.1}$$

Separating each dependent variable into mean and fluctuating parts, substituting into (8.1), and averaging then yields

$$\overline{\frac{Du}{Dt}} = \frac{\partial \bar{u}}{\partial t} + \frac{\partial}{\partial x}\left(\bar{u}\bar{u} + \overline{u'u'}\right) + \frac{\partial}{\partial y}\left(\bar{u}\bar{v} + \overline{u'v'}\right) + \frac{\partial}{\partial z}\left(\bar{u}\bar{w} + \overline{u'w'}\right) \tag{8.2}$$

Noting that the mean velocity fields satisfy the continuity equation (2.60), we can rewrite (8.2) as

$$\overline{\frac{Du}{Dt}} = \frac{\bar{D}\bar{u}}{Dt} + \frac{\partial}{\partial x}\left(\overline{u'u'}\right) + \frac{\partial}{\partial y}\left(\overline{u'v'}\right) + \frac{\partial}{\partial z}\left(\overline{u'w'}\right) \tag{8.3}$$

where

$$\frac{\overline{D}}{Dt} = \frac{\partial}{\partial t} + \overline{u}\frac{\partial}{\partial x} + \overline{v}\frac{\partial}{\partial y} + \overline{w}\frac{\partial}{\partial z}$$

is the rate of change following the mean motion. The mean equations thus have the form

$$\frac{\bar{D}\bar{u}}{Dt} = -\frac{1}{\rho_0}\frac{\partial \bar{p}}{\partial x} + f\bar{v} - \left[\frac{\partial \overline{u'u'}}{\partial x} + \frac{\partial \overline{u'v'}}{\partial y} + \frac{\partial \overline{u'w'}}{\partial z}\right] + \bar{F}_{rx} \tag{8.4}$$

$$\frac{\bar{D}\bar{v}}{Dt} = -\frac{1}{\rho_0}\frac{\partial \bar{p}}{\partial y} - f\bar{u} - \left[\frac{\partial \overline{u'v'}}{\partial x} + \frac{\partial \overline{v'v'}}{\partial y} + \frac{\partial \overline{v'w'}}{\partial z}\right] + \bar{F}_{ry} \tag{8.5}$$

$$\frac{\bar{D}\bar{w}}{Dt} = -\frac{1}{\rho_0}\frac{\partial \bar{p}}{\partial z} + g\frac{\bar{\theta}}{\theta_0} - \left[\frac{\partial \overline{u'w'}}{\partial x} + \frac{\partial \overline{v'w'}}{\partial y} + \frac{\partial \overline{w'w'}}{\partial z}\right] + \bar{F}_{rz} \tag{8.6}$$

$$\frac{\bar{D}\bar{\theta}}{Dt} = -\bar{w}\frac{d\theta_0}{dz} - \left[\frac{\partial \overline{u'\theta'}}{\partial x} + \frac{\partial \overline{v'\theta'}}{\partial y} + \frac{\partial \overline{w'\theta'}}{\partial z}\right] \tag{8.7}$$

$$\frac{\partial \bar{u}}{\partial x} + \frac{\partial \bar{v}}{\partial y} + \frac{\partial \bar{w}}{\partial z} = 0 \tag{8.8}$$

The various covariance terms in square brackets in (8.4) through (8.7) represent turbulent fluxes. For example, $\overline{w'\theta'}$ is a vertical turbulent heat flux in kinematic form. Similarly $\overline{w'u'} = \overline{u'w'}$ is a vertical turbulent flux of zonal momentum. For many boundary layers the magnitudes of the turbulent flux divergence terms are of the same order as the other terms in (8.4) through (8.7). In such cases, it is not possible to neglect the turbulent flux terms even when only the mean flow is of direct interest. Outside the boundary layer the turbulent fluxes are often sufficiently weak so that the terms in square brackets in (8.4) through (8.7) can be neglected in the analysis of large-scale flows. This assumption was implicitly made in Chapters 3 and 4.

The complete equations for the mean flow (8.4) through (8.8), unlike the equations for the total flow (2.56) through (2.60), and the approximate equations of Chapters 3 and 4, are not a closed set since in addition to the five unknown mean variables $\bar{u}, \bar{v}, \bar{w}, \bar{\theta}, \bar{p}$, there are unknown turbulent fluxes. To solve these equations, *closure* assumptions must be made to approximate the unknown fluxes in terms of the five known mean state variables. Away from regions with horizontal inhomogeneities (e.g., shorelines, towns, forest edges), we can simplify by assuming that the turbulent fluxes are horizontally homogeneous so that it is possible to neglect the horizontal derivative terms in square brackets in comparison to the terms involving vertical differentiation.

8.2 TURBULENT KINETIC ENERGY

Vortex stretching and twisting associated with turbulent eddies always tend to cause turbulent energy to flow toward the smallest scales, where it is dissipated by viscous diffusion. Thus, there must be continuing production of turbulence if the turbulent kinetic energy is to remain statistically steady. The primary source of boundary layer turbulence depends critically on the structure of the wind and temperature profiles near the surface. If the lapse rate is unstable, boundary layer turbulence is convectively generated. If it is stable, then instability associated with wind shear must be responsible for generating turbulence in the boundary layer. The comparative roles of these processes can best be understood by examining the budget for turbulent kinetic energy.

To investigate the production of turbulence, we subtract the component mean momentum equations (8.4) through (8.6) from the corresponding unaveraged equations (2.56), (2.57), and (2.58). We then multiply the results by u', v', w', respectively; add the resulting three equations; and average to obtain the turbulent kinetic energy equation. The complete statement of this equation is quite complicated, but its essence can be expressed symbolically as

$$\frac{\bar{D}\,(TKE)}{Dt} = MP + BPL + TR - \varepsilon \tag{8.9}$$

where $TKE \equiv (\overline{u'^2} + \overline{v'^2} + \overline{w'^2})/2$ is the turbulent kinetic energy per unit mass, MP is the mechanical production, BPL is the buoyant production or loss, TR designates redistribution by transport and pressure forces, and ε designates frictional dissipation. ε is always positive, reflecting the dissipation of the smallest scales of turbulence by molecular viscosity.

The buoyancy term in (8.9) represents a conversion of energy between mean flow potential energy and turbulent kinetic energy. It is positive for motions that lower the center of mass of the atmosphere and negative for motions that raise it. The buoyancy term has the form[1]

$$BPL \equiv \overline{w'\theta'}\,(g/\theta_0)$$

Positive buoyancy production occurs when there is heating at the surface so that an unstable temperature lapse rate (see Section 2.7.2) develops near the ground and spontaneous convective overturning can occur. As shown in the schematic of Figure 8.1, convective eddies have positively correlated vertical velocity and potential temperature fluctuations and hence provide a source of turbulent kinetic energy and positive heat flux. This is the dominant source in

[1] In practice, buoyancy in the boundary layer is modified by the presence of water vapor, which has a density significantly lower than that of dry air. The potential temperature should be replaced by virtual potential temperature in (8.9) in order to include this effect. (See, for example, Curry and Webster, 1999, p. 67.)

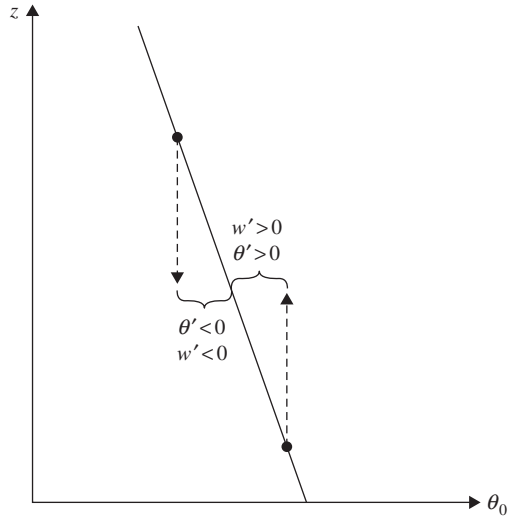

FIGURE 8.1 Correlation between vertical velocity and potential temperature perturbations for upward or downward parcel displacements when the mean potential temperature $\theta_0(z)$ decreases with height.

a convectively unstable boundary layer. For a statically stable atmosphere, *BPL* is negative, which tends to reduce or eliminate turbulence.

For both statically stable and unstable boundary layers, turbulence can be generated mechanically by dynamical instability due to wind shear. This process is represented by the mechanical production term in (8.9), which represents a conversion of energy between mean flow and turbulent fluctuations. This term is proportional to the shear in the mean flow and has the form

$$MP \equiv -\overline{u'w'}\frac{\partial \bar{u}}{\partial z} - \overline{v'w'}\frac{\partial \bar{v}}{\partial z} \tag{8.10}$$

MP is positive when the momentum flux is directed down the gradient of the mean momentum. Thus, if the mean vertical shear near the surface is westerly ($\partial\bar{u}/\partial z > 0$), then $\overline{u'w'} < 0$ for $MP > 0$.

In a statically stable layer, turbulence can exist only if mechanical production is large enough to overcome the damping effects of stability and viscous dissipation. This condition is measured by a quantity called the *flux Richardson number*. It is defined as

$$Rf \equiv -BPL/MP$$

If the boundary layer is statically unstable, then $\mathrm{Rf} < 0$ and turbulence is sustained by convection. For stable conditions, Rf will be greater than zero. Observations suggest that only when Rf is less than about 0.25 (i.e., mechanical

production exceeds buoyancy damping by a factor of 4) is the mechanical production intense enough to sustain turbulence in a stable layer. Since *MP* depends on the shear, it always becomes large close enough to the surface. However, as the static stability increases, the depth of the layer in which there is net production of turbulence shrinks. Thus, when there is a strong temperature inversion, such as produced by nocturnal radiative cooling, the boundary layer depth may be only a few decameters and vertical mixing is strongly suppressed.

8.3 PLANETARY BOUNDARY LAYER MOMENTUM EQUATIONS

For the special case of horizontally homogeneous turbulence above the viscous sublayer, molecular viscosity and horizontal turbulent momentum flux divergence terms can be neglected. The mean flow horizontal momentum equations (8.4) and (8.5) then become

$$\frac{\bar{D}\bar{u}}{Dt} = -\frac{1}{\rho_0}\frac{\partial \bar{p}}{\partial x} + f\bar{v} - \frac{\partial \overline{u'w'}}{\partial z} \tag{8.11}$$

$$\frac{\bar{D}\bar{v}}{Dt} = -\frac{1}{\rho_0}\frac{\partial \bar{p}}{\partial y} - f\bar{u} - \frac{\partial \overline{v'w'}}{\partial z} \tag{8.12}$$

In general, (8.11) and (8.12) can only be solved for $\overline{u}$ and $\overline{v}$ if the vertical distribution of the turbulent momentum flux is known. Because this depends on the structure of the turbulence, no general solution is possible. Rather, a number of approximate semiempirical methods are used.

For midlatitude synoptic-scale motions, Section 2.4 showed that to a first approximation the inertial acceleration terms—the terms on the left in (8.11) and (8.12)—can be neglected compared to the Coriolis force and pressure gradient force terms. Outside the boundary layer, the resulting approximation is then simply geostrophic balance. In the boundary layer the inertial terms are still small compared to the Coriolis force and pressure gradient force terms, but the turbulent flux terms must be included. Thus, to a first approximation, planetary boundary layer equations express a three-way balance among the Coriolis force, the pressure gradient force, and the turbulent momentum flux divergence:

$$f\left(\bar{v} - \bar{v}_g\right) - \frac{\partial \overline{u'w'}}{\partial z} = 0 \tag{8.13}$$

$$-f\left(\bar{u} - \bar{u}_g\right) - \frac{\partial \overline{v'w'}}{\partial z} = 0 \tag{8.14}$$

where (2.23) is used to express the pressure gradient force in terms of geostrophic velocity.

8.3.1 Well-Mixed Boundary Layer

If a convective boundary layer is topped by a stable layer, turbulent mixing can lead to formation of a well-mixed layer. Such boundary layers occur commonly over land during the day when surface heating is strong and over oceans when the air near the sea surface is colder than the surface water temperature. The tropical oceans typically have boundary layers of this type.

In a well-mixed boundary layer, the wind speed and potential temperature are nearly independent of height, as shown schematically in Figure 8.2, and to a first approximation it is possible to treat the layer as a slab in which the velocity and potential temperature profiles are constant with height and turbulent fluxes vary linearly with height. For simplicity, we assume that the turbulence vanishes at the top of the boundary layer. Observations indicate that the surface momentum flux can be represented by a *bulk aerodynamic formula*[2]:

$$\left(\overline{u'w'}\right)_s = -C_d \left|\overline{\mathbf{V}}\right| \bar{u}, \quad \text{and} \quad \left(\overline{v'w'}\right)_s = -C_d \left|\overline{\mathbf{V}}\right| \bar{v}$$

where C_d is a nondimensional *drag coefficient*, $|\overline{\mathbf{V}}| = h(\bar{u}^2 + \bar{v}^2)^{1/2}$, and the subscript s denotes surface values (referred to the standard anemometer height). Observations show that C_d is of order 1.5×10^{-3} over oceans, but may be several times as large over rough ground.

The approximate planetary boundary layer equations (8.13) and (8.14) can then be integrated from the surface to the top of the boundary layer at $z = h$

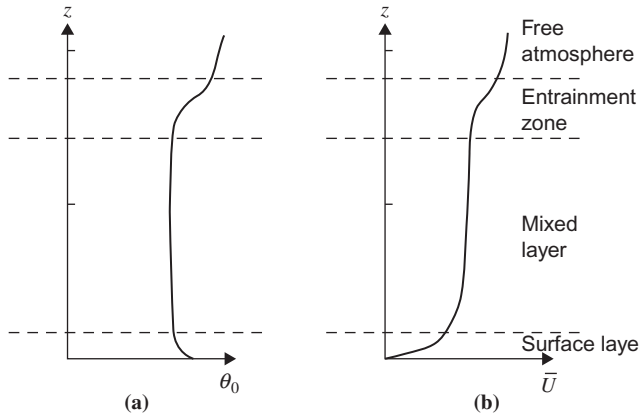

FIGURE 8.2 (a) Mean potential temperature, θ_0, and (b) mean zonal wind, U, profiles in a well-mixed boundary layer. (*Adapted from Stull, 1988.*)

[2]The turbulent momentum flux is often represented in terms of an "eddy stress" by defining, for example, $\tau_{ex} = \rho_o \overline{u'w'}$. We prefer to avoid this terminology to eliminate possible confusion with molecular friction.

to give

$$f\left(\bar{v}-\bar{v}_g\right)=-\left(\overline{u'w'}\right)_s/h=C_d\left|\overline{\mathbf{V}}\right|\bar{u}/h \tag{8.15}$$

$$-f\left(\bar{u}-\bar{u}_g\right)=-\left(\overline{v'w'}\right)_s/h=C_d\left|\overline{\mathbf{V}}\right|\bar{v}/h \tag{8.16}$$

Without loss of generality we can choose axes such that $\bar{v}_g = 0$. Then (8.15) and (8.16) can be rewritten as

$$\bar{v}=\kappa_s\left|\overline{\mathbf{V}}\right|\bar{u};\quad \bar{u}=\bar{u}_g-\kappa_s\left|\overline{\mathbf{V}}\right|\bar{v} \tag{8.17}$$

where $\kappa_s \equiv C_d/(fh)$. Thus, in the mixed layer the wind speed is less than the geostrophic speed and there is a component of motion directed toward lower pressure (i.e., to the left of the geostrophic wind in the Northern Hemisphere and to the right in the Southern Hemisphere) whose magnitude depends on κ_s. For example, if $\bar{u}_g = 10$ m s^{-1} and $\kappa_s = 0.05$ m^{-1} s, then $\bar{u} = 8.28$ m s^{-1}, $\bar{v} = 3.77$ m s^{-1}, and $\left|\overline{\mathbf{V}}\right| = 9.10$ m s^{-1} at all heights within this idealized slab mixed layer.

It is the work done by the flow toward lower pressure that balances the frictional dissipation at the surface. Because boundary layer turbulence tends to reduce wind speeds, the turbulent momentum flux terms are often referred to as boundary layer *friction*. It should be kept in mind, however, that the forces involved are due to turbulence, not molecular viscosity.

Qualitatively, the cross-isobar flow in the boundary layer can be understood as a direct result of the three-way balance among the pressure gradient force, the Coriolis force, and turbulent drag:

$$f\mathbf{k}\times\overline{\mathbf{V}}=-\frac{1}{\rho_0}\nabla\bar{p}-\frac{C_d}{h}\left|\overline{\mathbf{V}}\right|\overline{\mathbf{V}} \tag{8.18}$$

This balance is illustrated in Figure 8.3. Because the Coriolis force is always normal to the velocity and the turbulent drag is a retarding force, their sum can exactly balance the pressure gradient force only if the wind is directed toward lower pressure. Furthermore, it is easy to see that as the turbulent drag becomes increasingly dominant, the cross-isobar angle must increase.

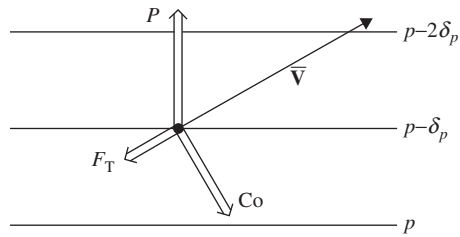

FIGURE 8.3 Balance of forces in the well-mixed planetary boundary layer: P designates the pressure gradient force; Co, the Coriolis force; and F_T, the turbulent drag.

8.3.2 The Flux–Gradient Theory

In neutrally or stably stratified boundary layers, the wind speed and direction vary significantly with height. The simple slab model is no longer appropriate; some means is needed to determine the vertical dependence of the turbulent momentum flux divergence in terms of mean variables in order to obtain closed equations for the boundary layer variables. The traditional approach to this closure problem is to assume that turbulent eddies act in a manner analogous to molecular diffusion so that the flux of a given field is proportional to the local gradient of the mean. In this case the turbulent flux terms in (8.13) and (8.14) are written as

$$\overline{u'w'} = -K_m\left(\frac{\partial \bar{u}}{\partial z}\right); \quad \overline{v'w'} = -K_m\left(\frac{\partial \bar{v}}{\partial z}\right)$$

and the potential temperature flux can be written as

$$\overline{\theta'w'} = -K_h\left(\frac{\partial \bar{\theta}}{\partial z}\right)$$

where $K_m(\mathrm{m^2\ s^{-1}})$ is the *eddy viscosity* coefficient and K_h is the eddy diffusivity of heat. This closure scheme is often referred to as the K theory.

The K theory has many limitations. Unlike the molecular viscosity coefficient, eddy viscosities depend on the flow rather than the physical properties of the fluid and must be determined empirically for each situation. The simplest models have assumed that the eddy exchange coefficient is constant throughout the flow. This approximation may be adequate for estimating the small-scale diffusion of passive tracers in the free atmosphere. However, it is a very poor approximation in the boundary layer where the scales and intensities of typical turbulent eddies are strongly dependent on the distance to the surface as well as the static stability. Furthermore, in many cases the most energetic eddies have dimensions comparable to the boundary layer depth, and neither the momentum flux nor the heat flux is proportional to the local gradient of the mean. For example, in much of the mixed layer, heat fluxes are positive even though the mean stratification may be very close to neutral.

8.3.3 The Mixing Length Hypothesis

The simplest approach to determining a suitable model for the eddy diffusion coefficient in the boundary layer is based on the mixing length hypothesis introduced by the famous fluid dynamicist Ludwig Prandtl. This hypothesis assumes that a parcel of fluid displaced vertically will carry the mean properties of its original level for a characteristic distance ξ' and then will mix with its surroundings just as an average molecule travels a mean free path before colliding and exchanging momentum with another molecule. By further analogy to the

molecular mechanism, this displacement is postulated to create a turbulent fluctuation whose magnitude depends on ξ' and the gradient of the mean property. For example,

$$\theta' = -\xi' \frac{\partial \bar{\theta}}{\partial z}; \quad u' = -\xi' \frac{\partial \bar{u}}{\partial z}; \quad v' = -\xi' \frac{\partial \bar{v}}{\partial z}$$

where it must be understood that $\xi' > 0$ for upward parcel displacement and $\xi' < 0$ for downward parcel displacement. For a conservative property, such as potential temperature, this hypothesis is reasonable provided that the eddy scales are small compared to the mean flow scale or that the mean gradient is constant with height. However, the hypothesis is less justified in the case of velocity, as pressure gradient forces may cause substantial changes in the velocity during an eddy displacement.

Nevertheless, if we use the mixing length hypothesis, the vertical turbulent flux of zonal momentum can be written as

$$-\overline{u'w'} = \overline{w'\xi'} \frac{\partial \bar{u}}{\partial z} \tag{8.19}$$

with analogous expressions for the momentum flux in the meridional direction and the potential temperature flux. In order to estimate w' in terms of mean fields, we assume that the vertical stability of the atmosphere is nearly neutral so that buoyancy effects are small. The horizontal scale of the eddies should then be comparable to the vertical scale so that $|w'| \sim |\mathbf{V}'|$ and we can set

$$w' \approx \xi' \left| \frac{\partial \overline{\mathbf{V}}}{\partial z} \right|$$

where $\mathbf{V}'$ and $\overline{\mathbf{V}}$ designate the turbulent and mean parts of the horizontal velocity field, respectively. Here the absolute value of the mean velocity gradient is needed because if $\xi' > 0$, then $w > 0$ (i.e., upward parcel displacements are associated with upward eddy velocities). Thus, the momentum flux can be written

$$-\overline{u'w'} = \overline{\xi'^2} \left| \frac{\partial \overline{\mathbf{V}}}{\partial z} \right| \frac{\partial \bar{u}}{\partial z} = K_m \frac{\partial \bar{u}}{\partial z} \tag{8.20}$$

where the eddy viscosity is now defined as $K_m = \overline{\xi'^2} \left| \partial \overline{\mathbf{V}} / \partial z \right| = \overline{\ell^2} \left| \partial \overline{\mathbf{V}} / \partial z \right|$ and the mixing length,

$$\ell \equiv \left(\overline{\xi'^2} \right)^{1/2}$$

is the root mean square parcel displacement, which is a measure of average eddy size. This result suggests that larger eddies and greater shears induce greater turbulent mixing.

8.3.4 The Ekman Layer

If the flux–gradient approximation is used to represent the turbulent momentum flux divergence terms in (8.13) and (8.14), and the value of K_m is taken to be constant, we obtain the equations of the classical Ekman layer:

$$K_m \frac{\partial^2 u}{\partial z^2} + f\left(v - v_g\right) = 0 \tag{8.21}$$

$$K_m \frac{\partial^2 v}{\partial z^2} - f\left(u - u_g\right) = 0 \tag{8.22}$$

where we have omitted the overbars because all fields are Reynolds-averaged.

The Ekman layer equations (8.21) and (8.22) can be solved to determine the height dependence of the departure of the wind field in the boundary layer from geostrophic balance. In order to keep the analysis as simple as possible, we assume that these equations apply throughout the depth of the boundary layer. The boundary conditions on u and v then require that both horizontal velocity components vanish at the ground and approach their geostrophic values far from the ground:

$$\begin{aligned} &u = 0,\ v = 0 \text{ at } z = 0 \\ &u \to u_g,\ v \to v_g \text{ as } z \to \infty \end{aligned} \tag{8.23}$$

To solve (8.21) and (8.22), we combine them into a single equation by first multiplying (8.22) by $i = (-1)^{1/2}$ and then adding the result to (8.21) to obtain a second-order equation in the complex velocity, $(u + iv)$:

$$K_m \frac{\partial^2 (u + iv)}{\partial z^2} - if\,(u + iv) = -if\left(u_g + iv_g\right) \tag{8.24}$$

For simplicity, we assume that the geostrophic wind is independent of height and that the flow is oriented so that the geostrophic wind is in the zonal direction ($v_g = 0$). Then the general solution of (8.24) is

$$(u + iv) = A \exp\left[(if/K_m)^{1/2} z\right] + B \exp\left[-(if/K_m)^{1/2} z\right] + u_g \tag{8.25}$$

It can be shown that $\sqrt{i} = (1 + i)/\sqrt{2}$. Using this relationship and applying the boundary conditions of (8.23), we find that for the Northern Hemisphere ($f > 0$), $A = 0$ and $B = -u_g$. Thus,

$$u + iv = -u_g \exp\left[-\gamma\,(1 + i)\, z\right] + u_g$$

where $\gamma = (f/2K_m)^{1/2}$.

Applying the Euler formula $\exp(-i\theta) = \cos\theta - i\sin\theta$ and separating the real from the imaginary part, we obtain for the Northern Hemisphere

$$u = u_g\left(1 - e^{-\gamma z}\cos\gamma z\right), \quad v = u_g e^{-\gamma z}\sin\gamma z \tag{8.26}$$

This solution is the famous Ekman spiral named for the Swedish oceanographer Vagn Walfrid Ekman, who first derived an analogous solution for the surface wind drift current in the ocean. The structure of the solution (8.26) is best illustrated by a hodograph as shown in Figure 8.4, where the zonal and meridional components of the wind are plotted as functions of height. The heavy solid curve traced out in Figure 8.4 connects all the points corresponding to values of u and v in (8.26) for values of γz increasing as one moves away from the origin along the spiral. Arrows show the velocities for various values of γz marked at the arrow points. When $z = \pi/\gamma$, the wind is parallel to and nearly equal to the geostrophic value. It is conventional to designate this level as the top of the Ekman layer and to define the layer depth as $De \equiv \pi/\gamma$.

Observations indicate that the wind approaches its geostrophic value at about 1 km above the surface. Letting $De = 1$ km and $f = 10^{-4}$ s^{-1}, the definition of γ implies that $K_m \approx 5$ m^2 s^{-1}. Referring back to (8.20), we see that for a characteristic boundary layer velocity shear of $|\delta\mathbf{V}/\delta z| \sim 5\times10^{-3}$ s^{-1}, this value of K_m implies a mixing length of about 30 m, which is small compared to the depth of the boundary layer, as it should be if the mixing length concept is to be useful.

Qualitatively, the most striking feature of the Ekman layer solution is that, like the mixed layer solution of Section 8.3.1, it has a boundary layer wind component directed toward lower pressure. As in the mixed layer case, this is a direct result of the three-way balance among the pressure gradient force, the Coriolis force, and the turbulent drag.

The ideal Ekman layer discussed here is rarely, if ever, observed in the atmospheric boundary layer. Partly this is because turbulent momentum fluxes are usually not simply proportional to the gradient of the mean momentum. However, even if the flux–gradient model were correct, it still would not be proper to assume a constant eddy viscosity coefficient, since in reality K_m must vary

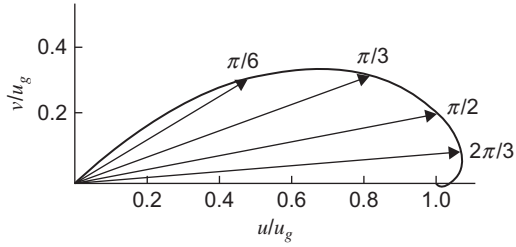

FIGURE 8.4 Hodograph of wind components in the Ekman spiral solution. *Arrows* show velocity vectors for several levels in the Ekman layer; the *spiral curve* traces out the velocity variation as a function of height. Points labeled on the spiral show the values of γz, which is a nondimensional measure of height.

rapidly with height near the ground. Thus, the Ekman layer solution should not be carried all the way to the surface.

8.3.5 The Surface Layer

Some of the inadequacies of the Ekman layer model can be overcome if we distinguish a *surface layer* from the remainder of the planetary boundary layer. The surface layer, whose depth depends on stability, but is usually less than 10% of the total boundary layer depth, is maintained entirely by vertical momentum transfer by the turbulent eddies; it is not directly dependent on the Coriolis or pressure gradient forces. Analysis is facilitated by supposing that the wind close to the surface is directed parallel to the x axis. The kinematic turbulent momentum flux can then be expressed in terms of a *friction velocity*, u_*, which is defined as[3]

$$u_*^2 \equiv \left|\overline{(u'w')_s}\right|$$

Measurements indicate that the magnitude of the surface momentum flux is of the order 0.1 $\mathrm{m^2\ s^{-2}}$. Thus, the friction velocity is typically of the order 0.3 $\mathrm{m\ s^{-1}}$.

According to the scale analysis in Section 2.4, the Coriolis and pressure gradient force terms in (8.11) have magnitudes of about 10^{-3} $\mathrm{m\ s^{-2}}$ in midlatitudes. The momentum flux divergence in the surface layer cannot exceed this magnitude or it would be unbalanced. Thus, it is necessary that

$$\frac{\delta\left(u_*^2\right)}{\delta z} \leq 10^{-3}\ \mathrm{m\ s^{-2}}$$

For $\delta z = 10$ m, this implies that $\delta(u_*^2) \leq 10^{-2}$ $\mathrm{m^2\ s^{-2}}$ so that the change in the vertical momentum flux in the lowest 10 m of the atmosphere is less than 10% of the surface flux.

To a first approximation it is then permissible to assume that in the lowest several meters of the atmosphere the turbulent flux remains constant at its surface value, so with the aid of (8.20),

$$K_m \frac{\partial \bar{u}}{\partial z} = u_*^2 \tag{8.27}$$

where we have parameterized the surface momentum flux in terms of the eddy viscosity coefficient. In applying K_m in the Ekman layer solution, we assumed a constant value throughout the boundary layer. Near the surface, however, the vertical eddy scale is limited by the distance to the surface. Thus, a logical choice for the mixing length is $\ell = kz$, where k is a constant. In that case

[3]Thus, the surface eddy stress (see footnote 3) is equal to $\rho_0 u_*^2$.

$K_m = (kz)^2 \left|\partial \bar{u} \,/\, \partial z\right|$. Substituting this expression into (8.27) and taking the square root of the result gives

$$\partial \bar{u} \,/\, \partial z = u_* / (kz) \tag{8.28}$$

Integrating with respect to z yields the *logarithmic wind profile*:

$$\bar{u} = \left(u_* \,/\, k\right) \ln \left(z \,/\, z_0\right) \tag{8.29}$$

where z_0, the *roughness length*, is a constant of integration chosen so that $\bar{u} = 0$ at $z = z_0$. The constant k in (8.29) is a universal constant called *von Karman's constant*, which has an experimentally determined value of $k \approx 0.4$. The roughness length z_0 varies widely depending on the physical characteristics of the surface. For grassy fields, typical values are in the range of 1 to 4 cm. Although a number of assumptions are required in the derivation of (8.29), many experimental programs have shown that the logarithmic profile provides a generally satisfactory fit to observed wind profiles in the surface layer.

8.3.6 The Modified Ekman Layer

As pointed out earlier, the Ekman layer solution is not applicable in the surface layer. A more satisfactory representation for the planetary boundary layer can be obtained by combining the logarithmic surface layer profile with the Ekman spiral. In this approach the eddy viscosity coefficient is again treated as a constant, but (8.24) is applied only to the region above the surface layer and the velocity and shear at the bottom of the Ekman layer are matched to those at the top of the surface layer. The resulting modified Ekman spiral provides a somewhat better fit to observations than the classical Ekman spiral. However, observed winds in the planetary boundary layer generally deviate substantially from the spiral pattern. Both transience and baroclinic effects (i.e., vertical shear of the geostrophic wind in the boundary layer) may cause deviations from the Ekman solution. However, even in steady-state barotropic situations with near neutral static stability, the Ekman spiral is seldom observed.

It turns out that the Ekman layer wind profile is generally unstable for a neutrally buoyant atmosphere. The circulations that develop as a result of this instability have horizontal and vertical scales comparable to the depth of the boundary layer. Thus, it is not possible to parameterize them by a simple flux–gradient relationship. However, these circulations do in general transport considerable momentum vertically. The net result is usually to decrease the angle between the boundary layer wind and the geostrophic wind from that characteristic of the Ekman spiral. A typical observed-wind hodograph is shown in Figure 8.5. Although the detailed structure is rather different from the Ekman spiral, the vertically integrated horizontal mass transport in the boundary layer is still directed toward lower pressure. As shown in the next section, this fact is of primary importance for synoptic- and larger-scale motions.

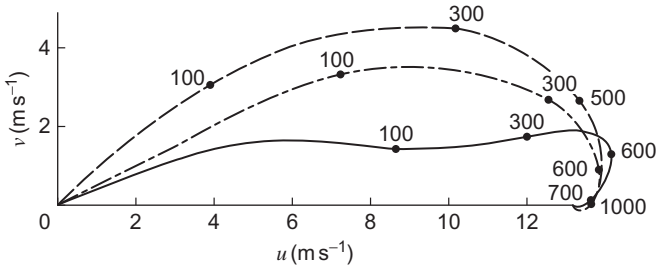

FIGURE 8.5 Mean wind hodograph for Jacksonville, Florida (≅30°N), April 4, 1968 (*solid line*) compared with the Ekman spiral (*dashed line*) and the modified Ekman spiral (*dash-dot line*) computed with $De \cong 1200$ m. Heights are shown in meters. (*Adapted from Brown, 1970. Copyright © American Meteorological Society. Reprinted with permission.*)

8.4 SECONDARY CIRCULATIONS AND SPIN DOWN

Both the mixed layer solution (8.17) and the Ekman spiral solution (8.26) indicate that in the planetary boundary layer the horizontal wind has a component directed toward lower pressure. As suggested by Figure 8.6, this implies mass convergence in a cyclonic circulation and mass divergence in an anticyclonic circulation, which by mass continuity requires vertical motion out of and into the boundary layer, respectively. To estimate the magnitude of this induced vertical motion, we note that if $v_g = 0$, the cross-isobaric mass transport per unit area at any level in the boundary layer is given by $\rho_0 v$. The net mass transport for a column of unit width extending vertically through the entire layer is simply the vertical integral of $\rho_0 v$. For the mixed layer, this integral is simply $\rho_0 vh$ (kg m^{-1} s^{-1}), where h is the layer depth. For the Ekman spiral, it is given by

$$M = \int_0^{De} \rho_0 v\, dz = \int_0^{De} \rho_0 u_g \exp(-\pi z/De) \sin(\pi z/De)\, dz \tag{8.30}$$

where $De = \pi/\gamma$ is the Ekman layer depth defined in Section 8.3.4.

Integrating the mean continuity equation (8.8) through the depth of the boundary layer gives

$$w(De) = -\int_0^{De} \left(\frac{\partial u}{\partial x} + \frac{\partial v}{\partial y} \right) dz \tag{8.31}$$

where we have assumed that $w(0) = 0$. Assuming again that $v_g = 0$ so that u_g is independent of x, we find after substituting from (8.26) into (8.31) and comparing with (8.30) that the mass transport at the top of the Ekman layer is

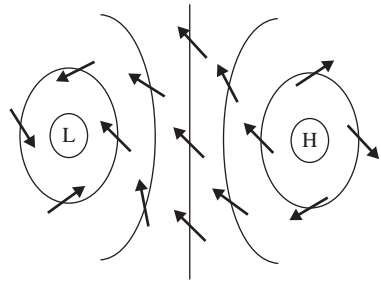

FIGURE 8.6 Schematic surface wind pattern (*arrows*) associated with high- and low-pressure centers in the Northern Hemisphere. Isobars are shown by thin lines, and "L" and "H" designate high- and low-pressure centers, respectively. (*After Stull, 1988.*)

given by

$$\rho_0 w(De) = -\frac{\partial M}{\partial y} \tag{8.32}$$

Thus, the mass flux out of the boundary layer is equal to the convergence of the cross-isobar mass transport in the layer. Noting that $-\partial u_g/\partial y = \zeta_g$ is just the geostrophic vorticity in this case, we find after integrating (8.30) and substituting into (8.32) that[4]

$$w(De) = \zeta_g \left(\frac{1}{2\gamma}\right) = \zeta_g \left|\frac{K_m}{2f}\right|^{1/2} \left(\frac{f}{|f|}\right) \tag{8.33}$$

where we have neglected the variation of density with height in the boundary layer and have assumed that $1 + e^{-\pi} \approx 1$. Thus, we obtain the important result that the vertical velocity at the top of the boundary layer is proportional to the geostrophic vorticity. In this way the effect of boundary layer fluxes is communicated directly to the free atmosphere through a forced *secondary circulation* that usually dominates over turbulent mixing. This process is often referred to as *boundary layer pumping*. It only occurs in rotating fluids and is one of the fundamental distinctions between rotating and nonrotating flow. For a typical synoptic-scale system with $\zeta_g \sim 10^{-5}\ \mathrm{s}^{-1}$, $f \sim 10^{-4}\ \mathrm{s}^{-1}$, and $De \sim 1$ km, the vertical velocity given by (8.33) is of the order of a few millimeters per second.

An analogous boundary layer pumping is responsible for the decay of the circulation created when a cup of tea is stirred. Away from the bottom and sides of the cup there is an approximate balance between the radial pressure gradient and the centrifugal force of the spinning fluid. However, near the bottom, viscosity slows the motion and the centrifugal force is not sufficient to

[4]The ratio of the Coriolis parameter to its absolute value is included so that the formula will be valid in both hemispheres.

balance the radial pressure gradient. (Note that the radial pressure gradient is independent of depth, since water is an incompressible fluid.) Therefore, radial inflow takes place near the bottom of the cup. Because of this inflow, the tea leaves are always observed to cluster near the center at the bottom of the cup if the tea has been stirred. By continuity of mass, the radial inflow in the bottom boundary layer requires upward motion and a slow compensating outward radial flow throughout the remaining depth of the tea. This slow outward radial flow approximately conserves angular momentum, and by replacing high angular momentum fluid with low angular momentum fluid, it makes the vorticity in the cup spin down far more rapidly than could mere diffusion.

The characteristic time for the secondary circulation to spin down an atmospheric vortex is illustrated most easily in the case of a barotropic atmosphere. For synoptic-scale motions, equation (4.38) can be written approximately as

$$\frac{D\zeta_g}{Dt} = -f\left(\frac{\partial u}{\partial x} + \frac{\partial v}{\partial y}\right) = f\frac{\partial w}{\partial z} \tag{8.34}$$

where we have neglected ζ_g compared to f in the divergence term and have also neglected the latitudinal variation of f. Recalling that the geostrophic vorticity is independent of height in a barotropic atmosphere, (8.34) can be integrated easily from the top of the Ekman layer ($z = De$) to the tropopause ($z = H$) to give

$$\frac{D\zeta_g}{Dt} = +f\left[\frac{w(H) - w(De)}{(H - De)}\right] \tag{8.35}$$

Substituting for $w(De)$ from (8.33), assuming that $w(H) = 0$ and that $H \gg De$, (8.35) may be written as

$$\frac{D\zeta_g}{Dt} = -\left|\frac{fK_m}{2H^2}\right|^{1/2}\zeta_g \tag{8.36}$$

This equation may be integrated in time to give

$$\zeta_g(t) = \zeta_g(0)\exp(-t/\tau_e) \tag{8.37}$$

where $\zeta_g(0)$ is the value of the geostrophic vorticity at time $t = 0$, and $\tau_e \equiv H|2/(fK_m)|^{1/2}$ is the time that it takes the vorticity to decrease to e^{-1} of its original value.

This *e-folding* time scale is referred to as the barotropic *spin-down time*. Taking typical values of the parameters as follows: $H \equiv 10\,\text{km}$, $f = 10^{-4}\ \text{s}^{-1}$, and $K_m = 10\ \text{m}^2\ \text{s}^{-1}$, we find that $\tau_e \approx 4$ days. Thus, for midlatitude synoptic-scale disturbances in a barotropic atmosphere, the characteristic spin-down time is a few days. This decay time scale should be compared to the time scale for ordinary viscous diffusion. For viscous diffusion the time scale can be estimated

from scale analysis of the diffusion equation

$$\frac{\partial u}{\partial t} = K_m \frac{\partial^2 u}{\partial z^2} \tag{8.38}$$

If τ_d is the diffusive time scale and H is a characteristic vertical scale for diffusion, then from the diffusion equation

$$U/\tau_d \sim K_m U/H^2$$

so that $\tau_d \sim H^2/K_m$. For the preceding values of H and K_m, the diffusion time scale is thus about 100 days. Thus, in the absence of convective clouds the spin-down process is a far more effective mechanism than eddy diffusion for destroying vorticity in a rotating atmosphere. Cumulonimbus convection can produce rapid turbulent transports of heat and momentum through the entire depth of the troposphere. These must be considered together with boundary layer pumping for intense systems such as hurricanes.

Physically the spin-down process in the atmospheric case is similar to that described for the teacup, except that in synoptic-scale systems it is primarily the Coriolis force that balances the pressure gradient force away from the boundary, not the centrifugal force. Again, the role of the secondary circulation driven by forces resulting from boundary layer drag is to provide a slow radial flow in the interior that is superposed on the azimuthal circulation of the vortex above the boundary layer. This secondary circulation is directed outward in a cyclone so that the horizontal area enclosed by any chain of fluid particles gradually increases. Since the circulation is conserved, the azimuthal velocity at any distance from the vortex center must decrease in time or, from another point of view, the Coriolis force for the outward-flowing fluid is directed clockwise, and this force thus exerts a torque opposite to the direction of the circulation of the vortex. Figure 8.7 shows a qualitative sketch of the streamlines of this secondary flow.

It should now be obvious exactly what is meant by the term *secondary circulation*. It is simply a circulation superposed on the primary circulation (in this case the azimuthal circulation of the vortex) by the physical constraints of the system. In the case of the boundary layer, viscosity is responsible for the presence of the secondary circulation. However, other processes, such as temperature advection and diabatic heating, may also lead to secondary circulations, as shown later.

The preceding discussion has concerned only the neutrally stratified barotropic atmosphere. An analysis for the more realistic case of a stably stratified baroclinic atmosphere is more complicated. However, qualitatively the effects of stratification may be easily understood. The buoyancy force (see Section 2.7.3) will act to suppress vertical motion, since air lifted vertically in a stable environment will be denser than the environmental air. As a result, the

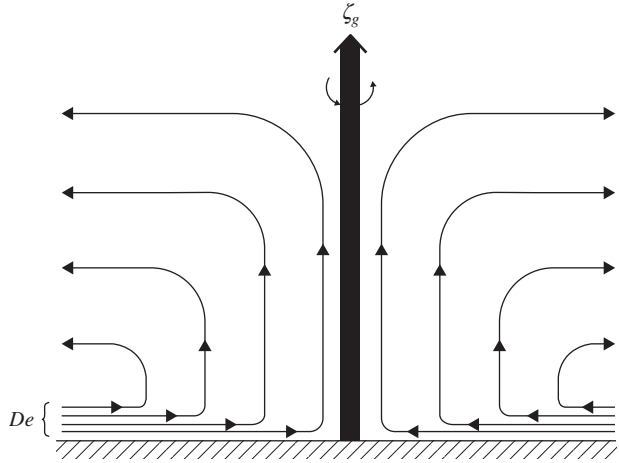

FIGURE 8.7 Streamlines of the secondary circulation forced by frictional convergence in the planetary boundary layer for a cyclonic vortex in a barotropic atmosphere. The circulation extends throughout the full depth of the vortex.

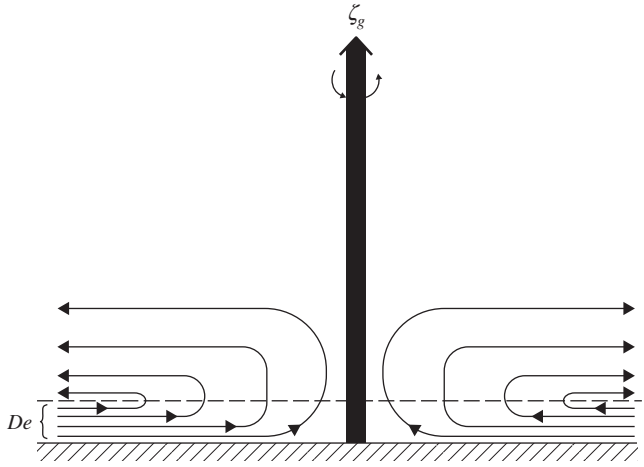

FIGURE 8.8 Streamlines of the secondary circulation forced by frictional convergence in the planetary boundary layer for a cyclonic vortex in a stably stratified baroclinic atmosphere. The circulation decays with height in the interior.

interior secondary circulation will decrease with altitude at a rate proportional to the static stability.

This vertically varying secondary flow, shown in Figure 8.8, will rather quickly spin down the vorticity at the top of the Ekman layer without appreciably affecting the higher levels. When the geostrophic vorticity at the top of the boundary layer is reduced to zero, the pumping action of the Ekman

layer is eliminated. The result is a baroclinic vortex with a vertical shear of the azimuthal velocity that is just strong enough to bring ζ_g to zero at the top of the boundary layer. This vertical shear of the geostrophic wind requires a radial temperature gradient that is in fact produced during the spin-down phase by adiabatic cooling of the air forced out of the Ekman layer. Thus, the secondary circulation in the baroclinic atmosphere serves two purposes: (1) it changes the azimuthal velocity field of the vortex through the action of the Coriolis force, and (2) it changes the temperature distribution so that a thermal wind balance is always maintained between the vertical shear of the azimuthal velocity and the radial temperature gradient.

SUGGESTED REFERENCES

Arya, *Introduction to Micrometeorology,* gives an excellent introduction to boundary layer dynamics and turbulence at the beginning undergraduate level.

Garratt, *The Atmospheric Boundary Layer*, is an excellent graduate-level introduction to the physics of the atmospheric boundary layer.

Stull, *An Introduction to Boundary Layer Meteorology*, provides a comprehensive and very nicely illustrated treatment of all aspects of the subject at the beginning graduate level.

PROBLEMS

8.1. Verify by direct substitution that the Ekman spiral expression (8.26) is indeed a solution of the boundary layer equations (8.21) and (8.22) for the case $v_g = 0$.

8.2. Derive the Ekman spiral solution for the more general case where the geostrophic wind has both x and y components (u_g and v_g, respectively), which are independent of height.

8.3. Letting the Coriolis parameter and density be constants, show that (8.33) is correct for the more general Ekman spiral solution obtained in Problem 8.2.

8.4. For laminar flow in a rotating cylindrical vessel filled with water (molecular kinematic viscosity $\nu = 0.01\ \mathrm{cm^2\ s^{-1}}$), compute the depth of the Ekman layer and the spin-down time if the depth of the fluid is 30 cm and the rotation rate of the tank is 10 revolutions per minute. How small would the radius of the tank have to be in order for the time scale for viscous diffusion from the side walls to be comparable to the spin-down time?

8.5. Suppose that at 43°N the geostrophic wind is westerly at 15 m $\mathrm{s^{-1}}$. Compute the net cross-isobaric transport in the planetary boundary layer using both the mixed layer solution (8.17) and the Ekman layer solution (8.26). You may let $|\mathbf{V}| = u_g$ in equation (8.17), $h = De = 1\ \mathrm{km}$, $\kappa_s = 0.015\ \mathrm{m^{-1}\ s}$, and $\rho = 1\ \mathrm{kg\,m^{-3}}$.

8.6. Derive an expression for the wind-driven surface Ekman layer in the ocean. Assume that the wind stress τ_w is constant and directed along the x axis. The continuity of turbulent momentum flux at the air–sea interface ($z = 0$)

requires that the wind stress divided by air density must equal the oceanic turbulent momentum flux at $z = 0$. Thus, if the flux–gradient theory is used, the boundary condition at the surface becomes

$$\rho_0 K \frac{\partial u}{\partial z} = \tau_w, \quad \rho_0 K \frac{\partial v}{\partial z} = 0, \quad \text{at } z = 0$$

where K is the eddy viscosity in the ocean (assumed constant). For a lower boundary condition, assume that $u, v \to 0$ as $z \to -\infty$. If $K = 10^{-3}$ m^2 s^{-1}, what is the depth of the surface Ekman layer at 43°N latitude?

8.7. Show that the vertically integrated mass transport in the wind-driven oceanic surface Ekman layer is directed 90° to the right of the surface wind stress in the Northern Hemisphere. Explain this result physically.

8.8. A homogeneous barotropic ocean of depth H = 3 km has a zonally symmetric geostrophic jet whose profile is given by the expression

$$u_g = U \exp\left[-(y/L)^2\right]$$

where $U = 1$ m s^{-1} and $L = 200$ km are constants. Compute the vertical velocity produced by convergence in the Ekman layer at the ocean bottom and show that the meridional profile of the secondary cross-stream motion forced in the interior is the same as the meridional profile of u_g. What are the maximum values of $\bar{v}$ in the interior and $\bar{w}$ if $K = 10^{-3}$ m^2 s^{-1} and $f = 10^{-4}$ s^{-1} (assume that w and the eddy stress vanish at the surface).

8.9. Using the approximate zonally averaged momentum equation

$$\frac{\partial \bar{u}}{\partial t} \cong f\bar{v}$$

compute the spin-down time for the zonal jet in Problem 8.8.

8.10. Derive a formula for the vertical velocity at the top of the planetary boundary layer using the mixed layer expression (8.17). Assume that $|\overline{\mathbf{V}}| = 5$ m s^{-1} is independent of x and y and that $\bar{u}_g = \bar{u}_g(y)$. If $h = 1$ km and $\kappa_s = 0.05$, what value must K_m have if this result is to agree with the vertical velocity derived from the Ekman layer solution at 43° latitude with $De = 1$ km?

8.11. Show that $K_m = kzu_*$ in the surface layer.

MATLAB Exercises

M8.1. The MATLAB script **mixed_layer_wind1.m** uses a simple iterative technique to solve for u and v in (8.17) with u_g in the range 1–20 m s^{-1} for the case $v_g = 0$ and $\kappa_s = 0.05$ m^{-1} s. If you run the script, you will observe that this iterative technique fails for u_g greater than 19 m s^{-1}. An alternative method, which works for a wide range of specified geostrophic winds, utilizes the natural coordinate system introduced in Section 3.2.1.

(a) Show that in the natural coordinate system the force balances parallel and perpendicular to the velocity vector in the mixed layer model (see Figure 8.3) can be expressed respectively as

$$f\kappa_s V^2 = f u_g \cos\beta \quad \text{and} \quad fV = f u_g \sin\beta$$

where it is assumed that the pressure gradient force is directed northward so that $fu_g = \left|\rho_0^{-1}\nabla p\right|$, and β designates the angle between the pressure gradient force vector and the mixed layer velocity, $\boldsymbol{V}$. (Other notation is as defined in Section 8.3.1.)

(b) Use MATLAB to solve for V and β given u_g in the range of 1 to $50\,\mathrm{m\,s^{-1}}$, and plot V and β versus u_g. *Hint*: Solve for V in the two equations in (a), and for each value of u_g, vary β until the two solutions for V agree.

M8.2. Suppose that the geopotential distribution at the top of the mixed layer can be expressed in the form $\Phi\,(x, y) = \Phi_0 - f_0 U_0 y + A\sin kx \sin ly$, where $\Phi_0 = 9800\,\mathrm{m^2\,s^{-2}}$, $f_0 = 10^{-4}\,\mathrm{s^{-1}}$, $U_0 = 5\,\mathrm{m\,s^{-1}}$, $A = 1500\,\mathrm{m^2\,s^{-2}}$, $k = \pi L^{-1}$, and, $l = \pi L^{-1}$, where $L = 6000\,\mathrm{km}$.

(a) Use the technique given in the demonstration script **mixed_layer_wind1.m** to determine the wind distribution in the mixed layer for this situation for the case where $\kappa_s = 0.05$.

(b) Using the formula obtained in Problem 8.10, compute the vertical velocity distribution at the top of the mixed layer for this distribution of geopotential when the depth of the mixed layer is 1 km. (The MATLAB script **mixed_layer_wind_2.m** has a template that you can use to contour the vertical velocity and the vorticity fields.)

M8.3. For the geopotential distribution of Exercise M8.2, use the Ekman layer theory to derive the pattern of vertical velocity at the top of the boundary layer. Assume that $K_m = 10\,\mathrm{m^2\,s^{-1}}$ and again use MATLAB to contour the fields of vorticity and vertical velocity. Explain why the vertical velocity patterns derived from the mixed layer and Ekman theories differ for this situation.